

MAJOR PAPER

Peripheral Retinal Leakage after Intravenous Administration of a Gadolinium-based Contrast Agent: Age Dependence, Temporal and Inferior Predominance and Potential Implications for Eye Homeostasis

Shinji Naganawa^{1*}, Rintaro Ito¹, Mariko Kawamura¹, Toshiaki Taoka¹,
Tadao Yoshida², and Michihiko Sone²

Purpose: Peripheral retinal leakage (PRL) of contrast medium from the ora serrata (i.e., the peripheral part of the retina) was recently reported in normal eyes using ultra-widefield fluorescein angiography. We occasionally see PRL of gadolinium-based contrast agents (GBCAs) in the vitreous from the temporal and inferior sides of the ora serrata on MR images of subjects without ophthalmic disease. In this study, we retrospectively evaluated these MR images to determine if PRL was associated with aging. We also evaluated whether the initial leakage appeared in the temporal and inferior sides, and whether there was uniform distribution within the vitreous after 24 hours.

Methods: In 127 subjects (9 volunteers, 85 patients with sudden deafness, and 33 patients with a suspicion of endolymphatic hydrops), pre- and post-contrast-enhanced heavily T2-weighted 3D-fluid attenuated inversion recovery (FLAIR) images were obtained. The presence or absence of PRL was subjectively evaluated. For patients with a suspicion of endolymphatic hydrops, 3D-real inversion recovery (IR) images were also obtained at pre-, 10 mins, 4 hours, and 24 hours after intravenous administration (IV) of GBCA. Four circular ROIs were placed in the vitreous humor and the signal intensity was measured.

Results: In the cases with PRL ($n = 88$) and without PRL ($n = 47$), the median age was 59 and 47 years, respectively ($P = 0.001$). At 4 hours after IV-GBCA, the mean signal increase in the inferior temporal ROI was greater than all the other ROIs. At 24 hours after IV-GBCA, no significant difference in signal intensity was observed for the four ROIs.

Conclusion: PRL of GBCA is age-dependent and occurs mainly from the inferior temporal side of the ora serrata. The contrast effect was uniformly distributed at 24 hours after IV-GBCA. Future observations in a variety of diseases will determine the clinical significance of these findings.

Keywords: *eye, gadolinium, glymphatic, magnetic resonance imaging, peripheral retinal leakage*

¹Department of Radiology, Nagoya University Graduate School of Medicine, Nagoya, Aichi, Japan

²Department of Otorhinolaryngology, Nagoya University Graduate School of Medicine, Nagoya, Aichi, Japan

*Corresponding author: Department of Radiology, Nagoya University Graduate School of Medicine, 65, Tsurumaicho, Shouwa-ku, Nagoya, Aichi 466-8550, Japan. Phone: +81-52-744-2327, Fax: +81-52-744-2335, E-mail: naganawa@med.nagoya-u.ac.jp;



This work is licensed under a Creative Commons Attribution-NonCommercial-NoDerivatives International License.

©2021 Japanese Society for Magnetic Resonance in Medicine

Received: July 15, 2021 | Accepted: September 4, 2021

Introduction

Peripheral retinal leakage (PRL), which is an extravascular leakage of contrast medium from the ora serrata (i.e. the peripheral part of the retina, Fig. 1), was a recently reported finding observed occasionally in normal eyes on ultra-wide-field fluorescein angiography (UWFA).^{1,2}

Since the contrast medium leaks at the far peripheral part of the retina, it is difficult to observe in a regular fundus examination. Therefore, the effect of aging on PRL and the relationship between PRL and various diseases are not well understood. PRL is a consequence of increased permeability of the blood-retinal barrier (BRB), which may affect the maintenance of homeostasis within the ocular environment.^{3,4}

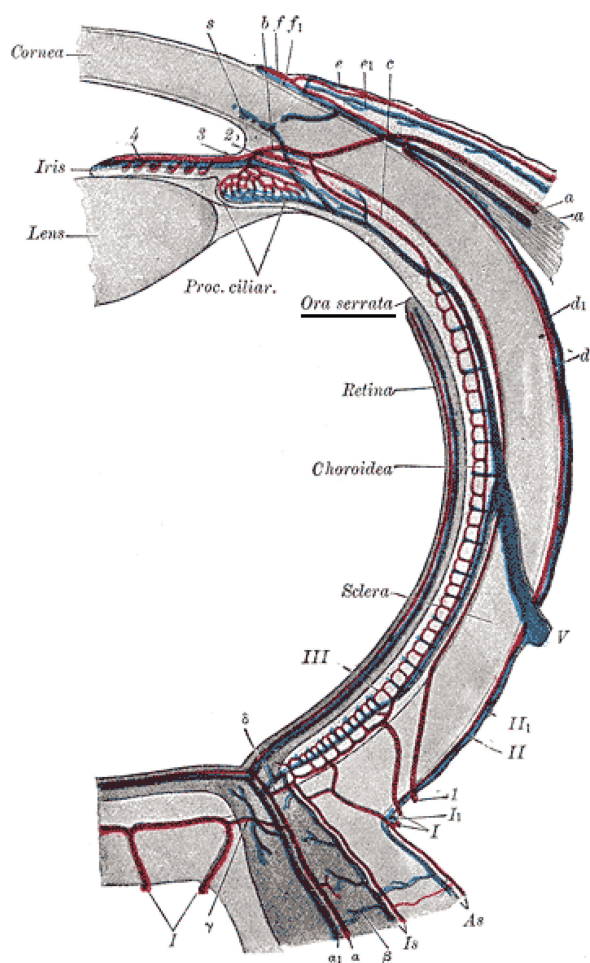


Fig. 1 Diagram of the blood vessels of the eye, as seen in a horizontal section reprinted from a textbook (Henry Gray. Anatomy of the human body, 1918. This diagram is open domain and freely downloadable at <https://commons.wikimedia.org/wiki/File:Gray877.png>) Ora serrata (underlined) is at the peripheral edge of the retina.

In Meniere's disease, the pulse sequences, which can detect low concentrations of gadolinium-based contrast agents (GBCAs) in the fluid, are used to evaluate endolymphatic hydrops in the inner ear.^{5,6} It has already been reported that these pulse sequences can be used to evaluate the migration of GBCA into the anterior aqueous and vitreous humors after intravenous administration (IV) of GBCA.^{7,8} In stroke patients, the permeation of GBCA into the vitreous has also been shown to be associated with aging, diabetes mellitus, and renal insufficiency in fluid attenuated inversion recovery (FLAIR) images obtained on the day after the IV-GBCA.⁹

On the images obtained for the evaluation of endolymphatic hydrops, in many patients immediately or 10 mins after IV-GBCA, punctate or band-like contrast leakage was observed occasionally from the retinal edge near the ora serrata, predominantly in the inferior part of the temporal side of the eye. We noted that this contrast enhancement often spread into the

vitreous after 4 hours and was almost uniformly distributed in the vitreous after 24 hours. Although it has been reported that surgery on the eye causes various imaging findings,^{10,11} we have observed the above-mentioned findings even in patients with no previous ocular surgery. To the best of our knowledge, there has been no report of punctate or band-like GBCA leakage on contrast-enhanced MRI from the peripheral part of the retina near the ora serrata in subjects without ocular diseases.

The purpose of this study was to retrospectively evaluate contrast-enhanced MR images to answer the following questions. (1) Is the frequency of appearance of this punctate or band-like contrast effect related to aging? (2) Does the vitreous contrast leakage spread from the temporal and inferior part of the peripheral region of the retina? (3) Does the vitreous contrast effect become uniform after 24 hours?

Materials and Methods

Subjects and GBCA

The subjects were healthy controls (HC), sudden deafness patients (SD), and suspected endolymphatic hydrops patients (EH) who underwent heavily T2-weighted 3D-FLAIR imaging before, and immediately after IV-GBCA. The total number of included subjects was 127, after excluding two patients with incomplete coverage of the eye due to an insufficient imaging field, and six patients with a history of bilateral lensectomy. The number of subjects, age range, median age, and number of male subjects of each group are as follows: HC, 9 subjects (29–53 years old, median: 38, 9 male subjects); SD, 85 patients (14–84 years old, median: 55, 46 male patients); EH, 33 patients (23–76 years old, median: 47, 17 male patients). In the EH group, the 3D-real inversion recovery (3D-real IR) sequence was also acquired at four time points: prior to, 10 mins, 4 hours, and 24 hours after IV-GBCA.

After the pre-contrast scan, a single dose (0.1 mmol/kg body weight) of intravenously administered (IV) gadoteridol (Pro-Hance; Eisai, Tokyo, Japan) was given to the HC group and a single dose (0.1 mmol/kg body weight) of IV gadobutrol (Gadovist; Bayer Yakuin, Osaka, Japan) to the SD and EH groups. No subjects in this study had an estimated glomerular filtration rate (eGFR) below 50 mL/min/1.73 m². No patients had obvious ophthalmic disease. However, we did not perform detailed ophthalmologic evaluations, such as visual acuity, intraocular pressure, fundus examination, and so on. No blood test information, such as blood glucose level or HbA1c, was obtained at the time of the examination.

MR imaging

A 3T MRI scanner (MAGNETOM Skyra; Siemens Healthineers, Erlangen, Germany) with a 32-channel head coil was used for all MR examinations. Heavily T2-weighted 3D-FLAIR was obtained using the following parameters: variable flip angle 3D-turbo spin-echo (sampling perfection

with application-optimized contrasts by the use of different flip angle evolutions [SPACE]): TR of 9000 msec; TE of 544 msec, inversion time of 2250 msec, initial refocusing 180° flip angle rapidly decreased to a constant 120° flip angle for the turbo spin-echo refocusing echo train; echo train length, 173; matrix size, 322 × 384; 104 axial slices with 1.0-mm-thick; FOV, 15 × 18 cm; generalized auto-calibrating partially parallel acquisition (GRAPPA) parallel imaging technique; acceleration factor, 2; number of excitations (NEX), 2; and scan time, 7 mins. The imaging slab covered the inner ear and eyes. The heavily T2-weighted 3D-FLAIR images were obtained before and immediately after IV-GBCA. Heavily T2-weighted MR cisternography was also obtained in the same slab orientation as heavily T2-weighted 3D-FLAIR. These parameters are similar to previous studies.^{7,12}

The 3D-real IR images were obtained in the EH group at pre-administration, and at 10 mins, 4 hours, and 24 hours after IV-GBCA using parameters that were similar to a previous study.¹³ Briefly, we obtained 256 axial slices with 1 mm thickness covering the entire brain using SPACE. The scan time for the 3D-real IR imaging was 10 mins per volume, with a TR of 15130 msec, TE of 549 msec, inversion time of 2700 msec, pixel size of 0.5 mm × 0.5 mm, 1 mm thickness, phase sensitive reconstruction (real reconstruction), acceleration factor of GRAPPA, 3, and NEX, 1.

Image analysis

All image analyses were performed on a picture archiving and communication systems (PACS) viewer (RapideyeCore; Canon Medical Systems, Tochigi, Japan) by an experienced neuroradiologist (S.N.). To evaluate the age dependency of the PRL, the presence or absence of punctate or band-like contrast enhancement on the vitreous surface at the temporal side of the eye was determined subjectively for all the three groups. When determining the presence or absence of the contrast enhancement, pre- and post-contrast heavily T2-weighted 3D-FLAIR images were compared.

As an objective evaluation of the GBCA leakage into the vitreous humor, the signal intensities were examined only in the EH group, in which pre-, 10-min, 4-hour and 24-hour imaging was also acquired with 3D-real IR. In the EH group, four circular ROIs with a diameter of 3 mm were placed in the vitreous humor of each eye on the axial slices of the lower and upper edge of the lens. We assigned the 12 o'clock position of the eye as the anterior edge of the cornea. In each slice, the center of the lateral (temporal) ROI was placed 3 mm from the 10 o'clock position (in the view from the foot) of the scleral inner surface to the center of the right eye. The center of the nasal ROI was placed 3 mm from the 2 o'clock position of the scleral inner surface to the center of the right eye. For the left eye, a temporal ROI was placed at the 2 o'clock position and nasal ROI was placed at the 10 o'clock position. Four ROIs (superior temporal [ST], superior nasal [SN], inferior temporal [IT], and inferior nasal [IN]) were placed on each eye according to the method described above.

The rationale for choosing the 2 o'clock and 10 o'clock positions was based on a previous anatomical review, which reported the average distance between the ora serrata and the equator of the eye to be 5.81 ± 1.12 mm on the nasal side and 6.00 ± 1.22 mm on the temporal side. This is 5.73 ± 0.81 mm on the nasal side and 6.53 ± 0.75 mm on the temporal side from Schwalbe's line (the outer limit of the corneal endothelium on the interior surface of the cornea) to the cornea.¹⁴ This approximately corresponds to the 10 o'clock and 2 o'clock positions when the eye is viewed from below and the anterior edge of the cornea is at 12 o'clock. Examples of the ROI locations are shown in Fig. 2.

As described above, four ROIs per eye (i.e., ST, SN, IT, and IN) were placed on the pre-contrast image, and then copied and pasted onto the three post-contrast phase images. For each subject, 8 ROIs (4 × 2 sides) × 4 time points = 32 ROIs were assessed. To evaluate the contrast effect, the signal increase was measured for each ROI by subtracting the signal value of the pre-contrast ROI from the signal value after contrast administration, and the results were compared for each time point and ROI location. The average signal value of each ROI was used for the subsequent evaluation.

On the 3D-real IR images used in the present study, the signal intensity of the brain parenchyma was nearly equal to zero. Therefore, we used the signal intensity values from the ROIs for the evaluation, instead of using signal ratio against a reference region such as the brain parenchyma. To verify that the fluctuation of the signal values between individuals was small, the coefficients of variation at the four locations were calculated for the signal values of the ROIs on the pre-contrast 3D-real IR images in the 66 eyes of the EH group.

For the HC and EH groups, the ethical committee of our institution approved this study. Written informed consent was obtained from all the participants. For the SD group, the imaging had been obtained in clinical practice, and written informed consent was waived by the ethics committee.

Statistical analysis

All the three groups were pooled, and the contrast enhancement of the lower temporal side of the eye was assessed subjectively. The age of the subjects with and without contrast enhancement was compared using a Mann-Whitney U test.

A comparison of the vitreous signal intensity for each ROI on the 3D-real IR images before IV-GBCA in the EH group was performed using an analysis of variance (ANOVA) with Bonferroni correction for multiple comparisons. The comparison of the signal increase from the pre-contrast images of the four ROIs in the vitreous of the EH group at each time point was performed using an ANOVA with Bonferroni correction for multiple comparisons. The comparison of the signal increase from the pre-contrast images for each ROI in the vitreous of the EH group between each time point was performed similarly using an ANOVA with Bonferroni correction for multiple comparisons.

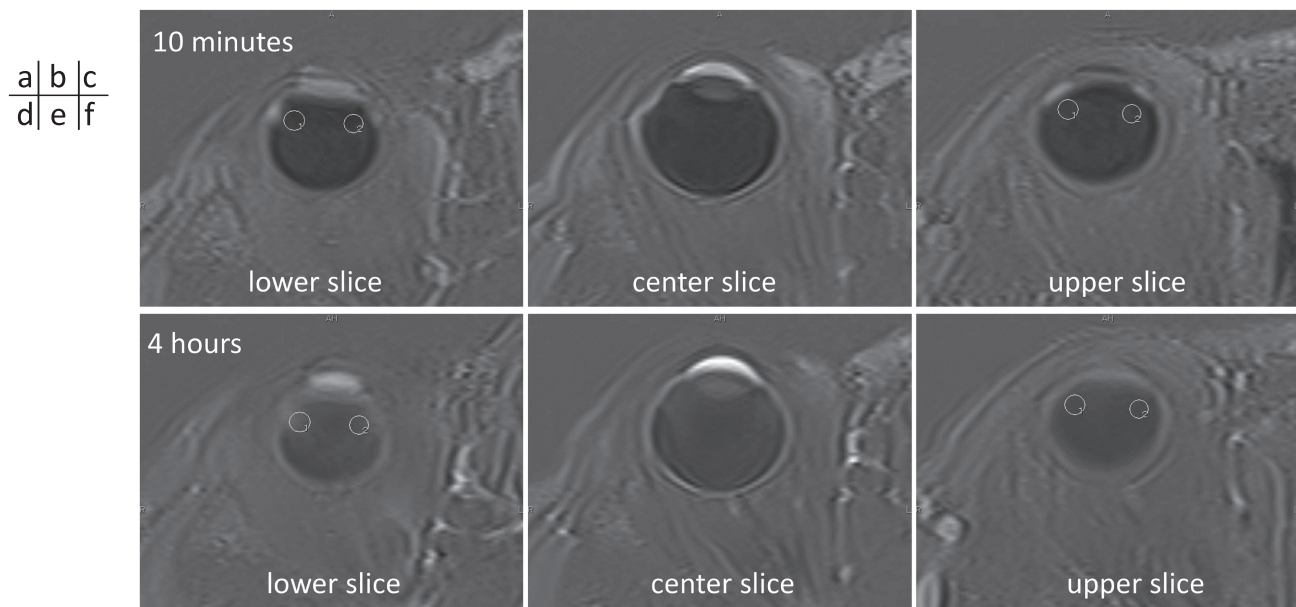


Fig. 2 Examples of the ROI locations in a 72-year-old woman with a suspicion of endolymphatic hydrops. Enlarged views of the axial 3D-real IR images for the right eye are shown. The images were obtained at 10 mins (a–c) and 4 hours (d–f) after IV-GBCA. Slices in the lower edge of the lens (a and d), slices in the center of the lens (b and e), and slices in the upper edge of the lens (c and f) are shown. Four circular ROIs with a diameter of 3 mm were placed in the vitreous humor of each eye on the axial slices of the upper and lower edges of the lens. We assigned the 12 o'clock position of the eye as the top of the cornea. In each slice, the center of the temporal ROI (circles #1) was placed 3 mm from the 10 o'clock position of the scleral inner surface to the center of the right eye. The center of the nasal ROI (circles #2) was placed 3 mm from the 2 o'clock position of the scleral inner surface to the center of the right eye. For the left eye, temporal ROI was placed at the 2 o'clock position and nasal ROI was placed at the 10 o'clock position. Four ROIs (superior temporal, superior nasal, inferior temporal, and inferior nasal) were placed in each eye according to the method described above to measure the signal intensity. Note that the lower temporal ROI at 4 hours after IV-GBCA (circle #1 in d) contains the most intensely enhanced area of the right eye in this patient. GBCA, gadolinium-based contrast agent; IR, inversion recovery; IV, intravenous administration.

To evaluate the relationship between the subjective assessment of enhancement and the objective assessment of enhancement in EH group, we compared the objective signal intensity increase at 4 hours from baseline of the inferior temporal (IT) ROI between the negative and positive groups for the subjective assessment of punctate or band-like enhancement using a Mann–Whitney U test.

We used 5% as a threshold to determine statistical significance. The software R (version 3.3.2; R Foundation for Statistical Computing, Vienna, Austria, <https://www.R-project.org/>) was used for the statistical analyses.

Results

Subjective evaluation in all groups

On pre-contrast heavily T2-weighted-3D-FLAIR imaging, there was no punctate or band-like high signal intensities in any of the eyes. Immediately after the contrast administration, the heavily T2-weighted-3D-FLAIR image showed a punctate or a band-like high signal in 6 eyes (3 of 9 subjects) in the HC group, 42 eyes (21 of 85 patients) in the SD group, and 28 eyes (14 of 33 patients) in EH group (Fig. 3). All regions of high intensity were seen in both eyes, and none were seen in only one eye. All three groups were pooled and

the median age was 59 years old for the cases with contrast enhancement ($n = 88$) and 47 years old for those without contrast enhancement ($n = 47$) in the lower temporal side of the eye ($P = 0.001$) (Fig. 4).

Objective evaluation of the pre-contrast images in the EH group

The mean signal intensities, standard deviations, and coefficients of variation of the vitreous enhancement in 33 cases (66 eyes) for each ROI on the pre-contrast 3D-real IR images are shown in Table 1.

The coefficients of variation of the vitreous signal intensity on the pre-contrast 3D-real IR images among subjects were -0.0133 in the IT ROI, -0.139 in the superior temporal (ST) ROI, -0.122 in the superior nasal (SN) ROI, and -0.121 in the inferior nasal (IN) ROI. A comparison of the mean signal intensity of the ROIs at the four sites showed that the IT was higher than the ST and SN, but the other pairs were not significantly different.

Objective evaluation of contrast enhancement in the EH group

Representative serial 3D-real IR images before and after IV-GBCA are shown in Fig. 5. The results of the signal intensity

a	b
c	d
e	f
g	h

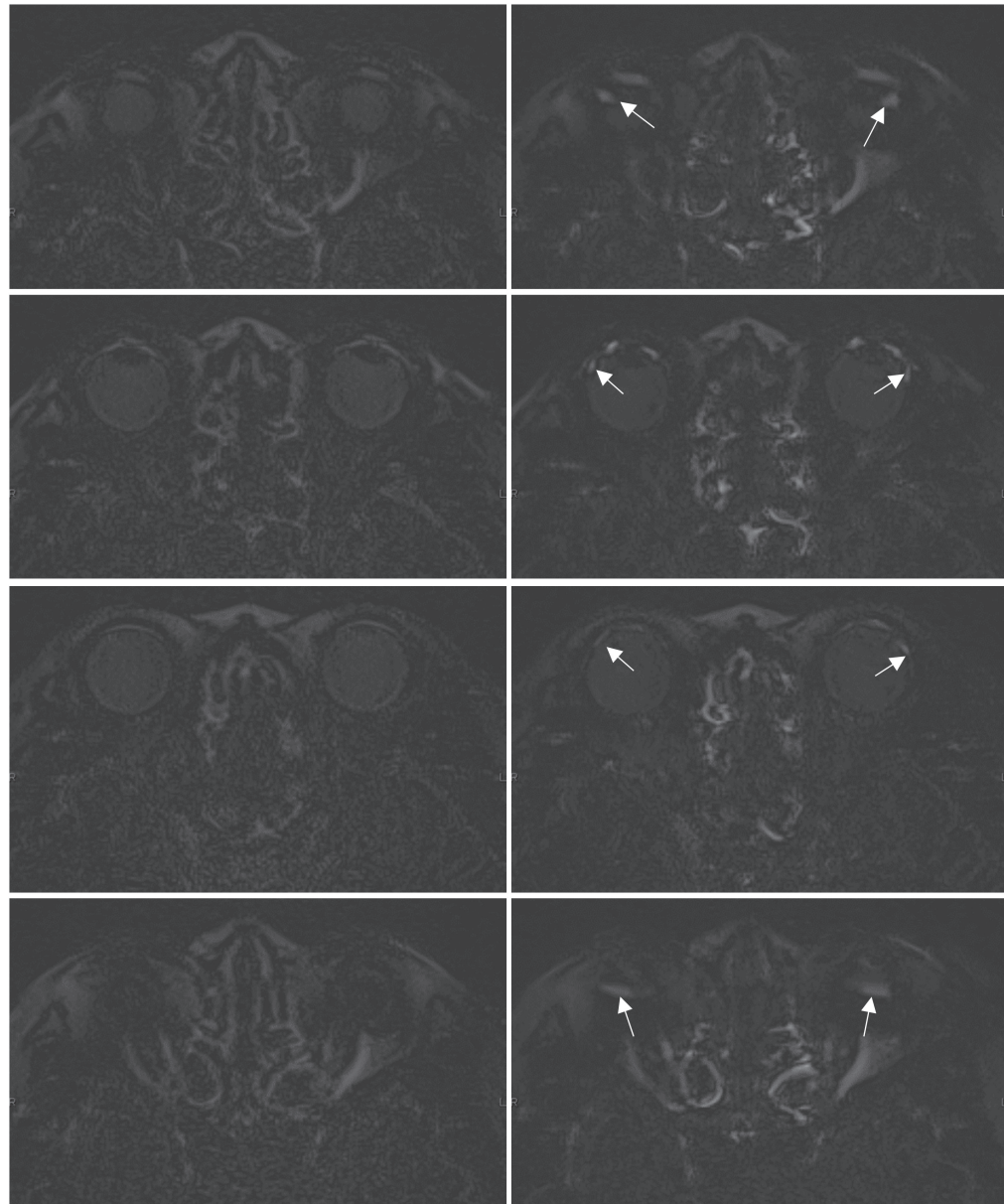


Fig. 3

(Continued)

increase in the four ROIs at each time phase after IV-GBCA are shown in Fig. 6. At 10 mins after IV-GBCA, the mean signal intensity increase in the IT was higher than that in the ST and SN (Fig. 6a). At 4 hours after IV-GBCA, the mean signal intensity increase in the IT was higher than all other ROIs (Fig. 6b). At 24 hours after IV-GBCA, no significant difference was observed among the signal intensity increases in the four ROIs (Fig. 6c).

The temporal trend of the signal intensity increase in each ROI is shown in Fig. 7. In all ROIs, the signal intensity increase was significantly higher at 4 and 24 hours than at pre- and 10 mins post- IV-GBCA.

The objective signal intensity increase at 4 hours from baseline of IT ROI was significantly larger in the patients

with the finding of the subjective assessment of punctate or band-like enhancement than those without ($P < 0.0001$). The average \pm standard deviation of signal increase was 14.0 ± 10.8 in the negative group (38 eyes) and 37.1 ± 24.1 in the positive group (28 eyes).

Discussion

In the present study using IV-GBCA, the following findings were observed. PRL was predominant in the inferior temporal side of the peripheral side of the retina. PRL increased with age. The distribution of GBCA in the vitreous humor became uniform after 24 hours. The pre-contrast signal

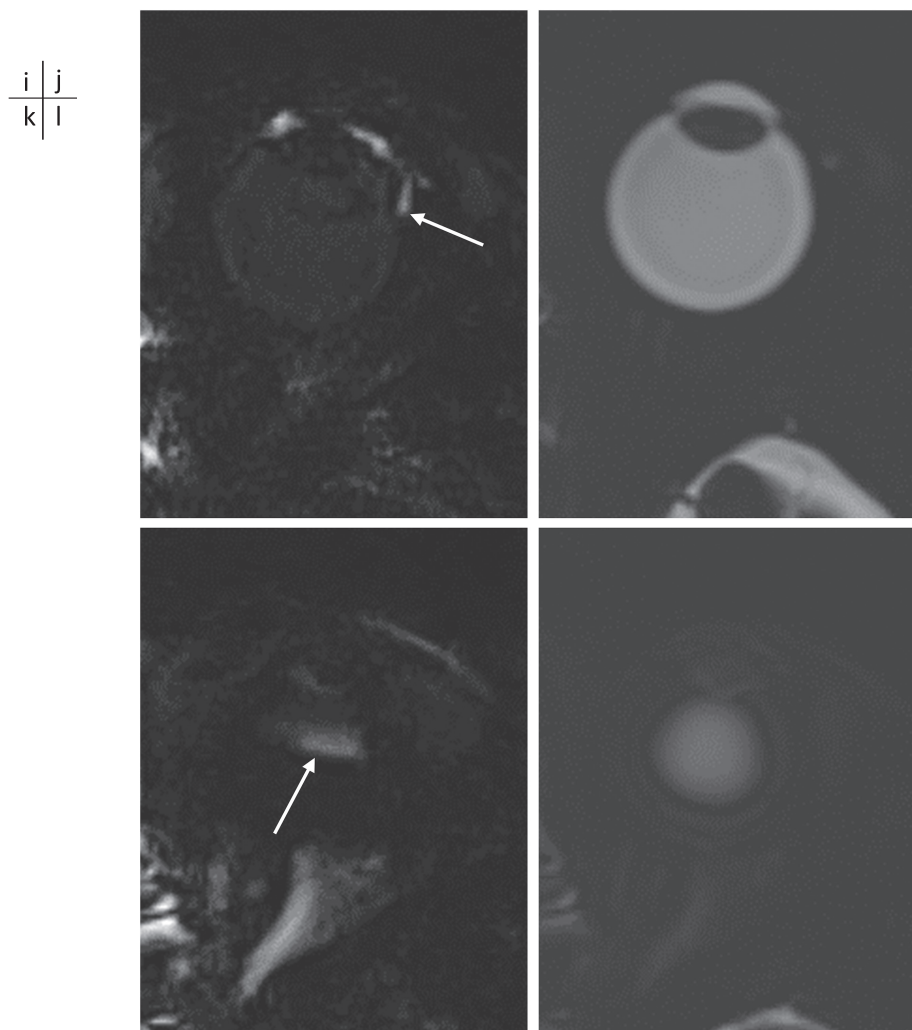


Fig. 3 Heavily 3D-FLAIR images obtained at pre- (**a**, **c**, **e**, and **g**) and immediately after (**b**, **d**, **f**, and **h**) IV-GBCA in a 72-year-old woman with right sudden hearing loss. Axial slices in the upper level of the lens edge (**a** and **b**), slices at the level of the center of the lens (**c** and **d**), slices in the lower level of the edge of the lens (**e** and **f**), and slices in the farthest lower level of the eye (**g** and **h**). In both eyes, punctate or band-like-shaped GBCA leakage to the vitreous from the vicinity of the ora serrata is observed mainly on the temporal side (arrows in **b**, **d**, **f**, and **h**). Enlarged views of the left eye are shown (**i**–**l**). (**i**) is corresponding to (**d**). (**j**) is MR cisternography at the same position of (**i**). (**k**) is corresponding to (**h**). (**l**) is MR cisternography at the same position of (**k**). In these enlarged views, the finding that the punctate or band-like-shaped GBCA leakage is protruding to the vitreous from the vicinity of the ora serrata can be more conspicuously appreciated (arrows in **i** and **k**). GBCA, gadolinium-based contrast agent; IV, intravenous administration.

intensity was highest in the ROI of the IT. It is assumed that molecules other than GBCA also might leak to the vitreous.

It remains unknown why PRL was observed predominantly in the inferior temporal side. Apart from normal physiological conditions, it has been reported that fluorescein leakage was most remarkable at the temporal sector of the ora serrata using fluorescein angiography of the peripheral retina and the pars plana during a vitrectomy for proliferative diabetic retinopathy.¹⁵

Anatomically, the distance from the optic papilla is larger on the temporal side of the ora serrata than on the nasal side. Therefore, the blood vessels on the temporal side of the

peripheral retina are more susceptible to ischemia than on the nasal side. This difference in the distance from the optic papilla might be the cause for the predominance of PRL on the temporal side. As for the difference between the superior and inferior sides, we do not have a concrete answer. Gravity might affect the leakage; however, the reason for the predominance on the inferior side remains unclear. Furthermore, causes of the degree of contrast leakage and its distribution possibly relating to pathological conditions other than aging (e.g., prolongation of the ocular axis due to intense myopia, vascular damage due to diabetes mellitus, intraocular pressure, poor function of the ocular glymphatic system, etc.) are

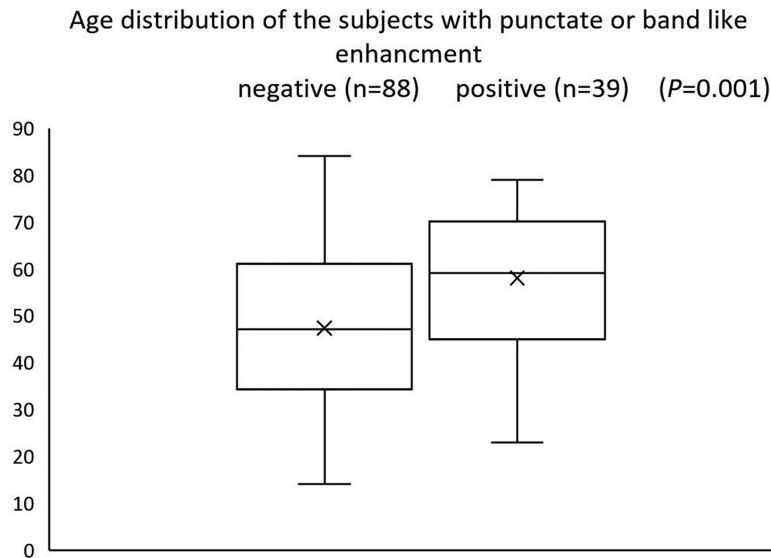


Fig. 4 A box-and-whisker plot of the age distribution of the GBCA leakage for the negative and positive groups. The age distribution overlaps between the two groups; however, the difference is significant ($P = 0.001$). Median age of the leakage positive group is higher than that of the negative group. In the box-and-whisker plot, the lower side of the rectangle is the first quartile (25th percentile value) and the upper side is the 75th percentile value. The horizontal line in the rectangle is the median. The cross in the rectangle under the whisker indicates the minimum value, and the horizontal line above the whisker indicates the maximum value. GBCA, gadolinium-based contrast agent.

Table 1 Signal intensity values of each ROI in pre-contrast 3D-real IR

	Mean		Standard deviation	Coefficients of variation
IT	-49.455	*, **	6.594	-0.133
ST	-53.667	*	7.480	-0.139
SN	-53.212	**	6.461	-0.121
IN	-50.924		6.225	-0.122

*and ** indicate significant difference. We used 5% as a threshold. IN, inferior nasal; IT, inferior temporal; SN, superior nasal; ST, superior temporal.

subjects for future research. The results of this study might suggest research directions for many future studies.

Using UWFA, it was reported that granular background fluorescence appeared in 100%, a mottled fluorescent band appeared in 43.6%, and retinal vascular leakage appeared in 19.8% of normal eyes in far peripheral retina.¹ Another study reported the appearance of a mottled fluorescent band in the far peripheral retina in 42.17%, ground glass hyper fluorescence in 85.34%, and late-phase slight leakage in 32.53% of normal eyes.² The mottled fluorescent band can occur with vascular leakage simultaneously or separately.¹ The molecular weight of fluorescein is 389.38 g/mol. It is reasonable that we could detect a similar leakage of GBCA at the peripheral part of normal eyes similar to the UWFA results, using the highly sensitive pulse sequences of this present study.

Some normal eyes show PRL and other normal eyes do not, as found by the present study, as well as the studies using UWFA. It is speculated that PRL might cause an alteration in the homeostasis of the vitreous humor.^{3,4} A further study to reveal the predictive values of PRL under various pathological conditions would be warranted in the future. As in

Alzheimer's disease, normal pressure hydrocephalus, Meniere's disease, and other brain diseases, the glymphatic system is presumed to be involved in the neurodegeneration, as well as in glaucoma disease.^{16,17} Contrast-enhanced MRI is a promising tool to evaluate ocular homeostasis, including the state of the BRB and the waste clearance system in the eye. Contrast-enhanced MRI might be able to simultaneously evaluate the eye, the inner ear, and the whole brain, regarding their vascular permeabilities and the waste clearance functions.¹⁸

There are several limitations to this study. Patients with sudden hearing loss and endolymphatic hydrops were included in the study, as well as healthy subjects. The effect of these diseases on the eye is not known, but patients with obvious ophthalmic diseases were not included. Multivariate analysis that includes not only age but also other factors such as the degree of endolymphatic hydrops and gender might be needed in the future. The present study did not quantify the signal ratio or a T1 value but evaluated the 3D-real IR signal intensity itself. In the evaluation of MR signal intensities, the intensity of a reference region, such as the brain parenchyma, is often used, where the signal is not expected to change before and after contrast. However, since the 3D-real IR imaging used in this study is heavily T2-weighted, the signal intensity of the brain parenchyma is close to zero, and the intensity ratio tends to fluctuate when it is used as the denominator. In this study, the receiver gain was fixed, and the distance from the coil element to the ROIs did not change much between phases. Therefore, using the signal intensity itself is considered a reasonable, though not ideal, method. The same method has been used in previous studies.¹⁸ The signal intensity of each ROI of the vitreous humor on the pre-contrast 3D-real IR images was measured and compared among the four ROIs. In each ROI, the coefficients of variation in 66 eyes were small (0.121–0.139). These small

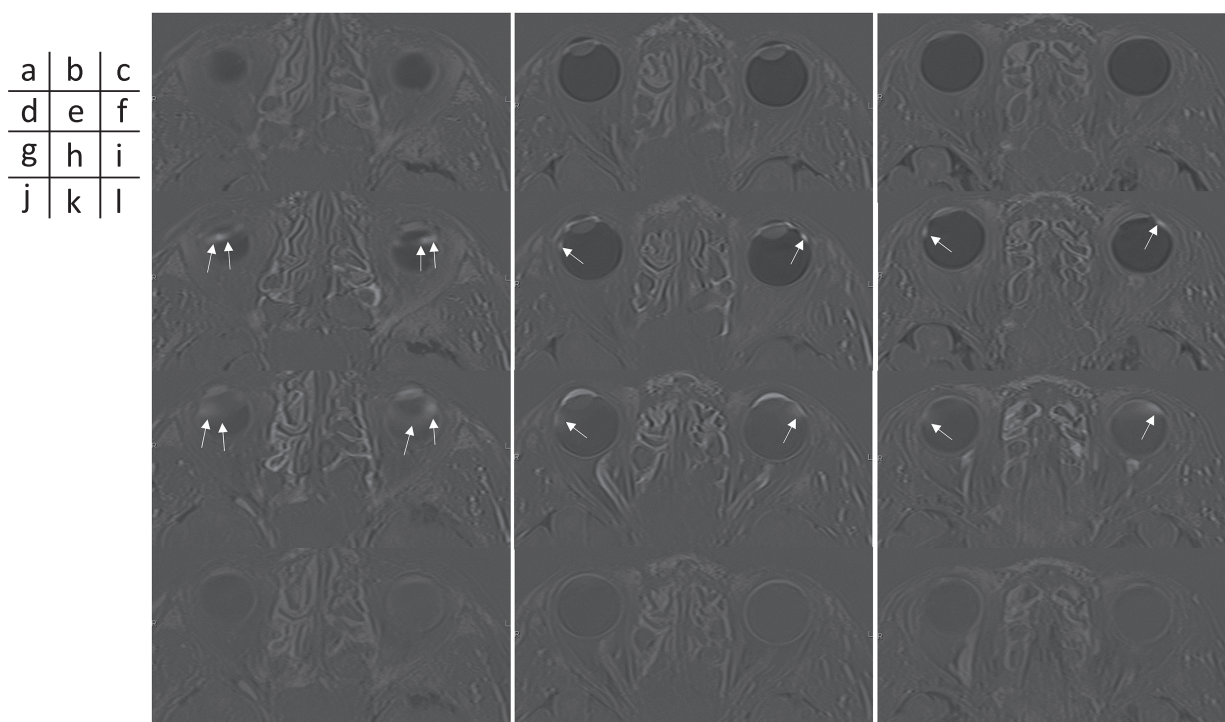


Fig. 5 The 3D-real IR images obtained at pre- (**a–c**) and 10 mins (**d–f**), 4 hours (**g–i**), and 24 hours (**j–l**) after IV-GBCA in a 76-year-old woman with a suspicion of endolymphatic hydrops. Axial slices in the lower level of the lens edge (**a**, **d**, **g**, and **j**), slices at the level of the center of lens (**b**, **e**, **h**, and **k**), and slices in the upper level of the edge of the lens (**c**, **f**, **i**, and **l**). In both eyes, punctate or band-like-shaped GBCA leakage into the vitreous from the vicinity of the ora serrata is observed mainly on the temporal side (arrows in **d–f**) at 10 mins after IV-GBCA. The enhancement in the lower side seems to be predominant (**d** and **g**). The enhancement spread into the vitreous at 4 hours after IV-GBCA (arrows in **g–i**). At 24 hours after IV-GBCA, uniform enhancement of the vitreous can be observed (**j–l**). GBCA, gadolinium-based contrast agent; IR, inversion recovery; IV, intravenous administration.

coefficients of variation in the pre-contrast images indicate the validity and stability of the signal intensities. The mean intensity in the IT was higher than that of the ST and SN. It is speculated that the increased permeability in the inferior temporal area might contribute to the higher signal intensity of the vitreous due to leaked solutes, such as proteins in the blood plasma.

The contrast agent was not standardized among the three groups. Gadoteridol was used for the HC group and gadobutrol for the other groups. The molecular weights of gadoteridol (558.7 g/mol) and gadobutrol (604.71 g/mol) are similar. The analysis including the two contrast agents was done only for the subjective evaluation of the presence and absence of contrast leakage among the three groups. The objective signal intensity measurements were performed only for the EH group using gadobutrol. A comparison between the two contrast agents was not included in the results of the present study. Thus, it is assumed that the effect using two different contrast agents might be small regarding the results.

Since the 3D-real IR and 24-hour post-contrast images were obtained only in the EH group, the number of cases for the objective evaluation was small. We excluded patients

with a history of ophthalmic surgery. However, the significance of the results is limited by a lack of detailed ophthalmological findings (intraocular pressure, visual acuity, anterior aqueous humor protein concentration, and findings of the fundus examination) and a lack of biometric information such as HbA1c and blood pressure at the time of the MR examination. The direct comparison between the contrast enhancement in MR imaging and UWFA would be necessary to confirm the precise leakage point of GBCA in the future.

Conclusion

In this preliminary study, we found, for the first time, that intravenously injected gadolinium contrast agent leaks into the vitreous humor from the ora serrata in normal eyes. This contrast leakage into the vitreous is age-dependent and occurs mainly from the inferior temporal side of the eye. The contrast effect is uniformly distributed at 24 hours after the contrast administration. Currently, the reason for the contrast leakage in the inferior temporal side remains unknown. Future observations in a variety of diseases will determine the clinical significance of these findings.

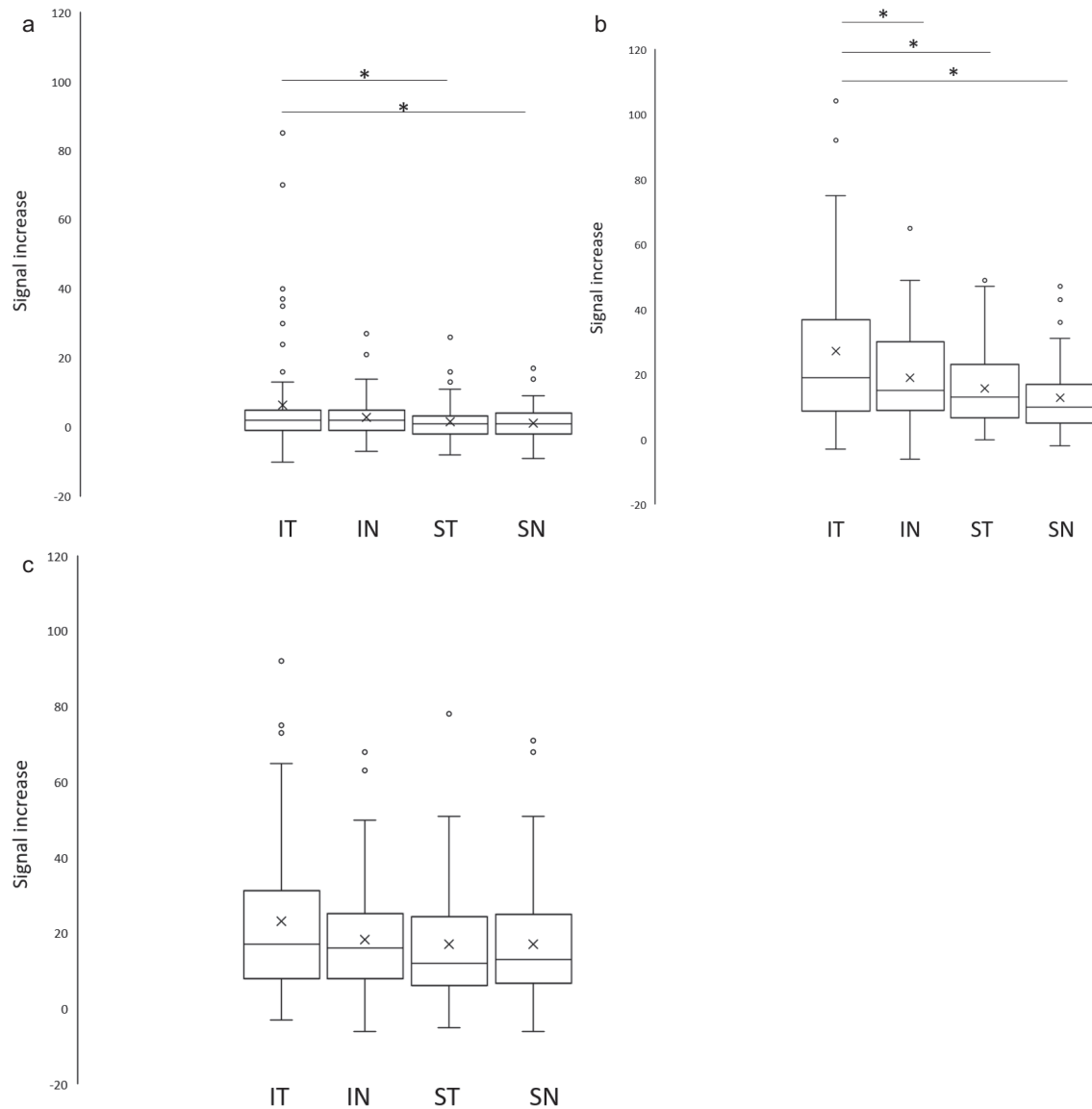


Fig. 6 The signal increase was measured in the 3D-real IR images obtained before, 10 mins, 4 hours, and 24 hours after IV-GBCA in the 33 patients with a suspicion of endolymphatic hydrops. Four ROIs (IT, IN, ST, and SN) was placed in 66 eyes of 33 patients. In the box-and-whisker plot, the lower side of the rectangle is the first quartile (25th percentile value) and the upper side is the 75th percentile value. The horizontal line in the rectangle is the median. The cross shows the mean. The horizontal line under the whisker indicates the lower extreme value, and the horizontal line above the whisker indicates the upper extreme value. The upper extreme and the lower extreme are 1.5x IQR away from the edge of the box. Small circles above the whiskers are outliers. We used 5% as a threshold to determine statistical significance. **(a)** A box-and-whisker plot for the distribution of the signal increase in the four ROIs at 10 mins after IV-GBCA. The signal increase in the IT is significantly higher than that in the ST and SN. **(b)** A box-and-whisker plot for the distribution of the signal increase in the four ROIs at 4 hours after IV-GBCA. The signal increase in the IT is significantly higher than all other ROIs. **(c)** A box-and-whisker plot for the distribution of the signal increase in the four ROIs at 24 hours after IV-GBCA. There was no significant difference between the four ROIs. *: Significant difference. GBCA, gadolinium-based contrast agent; IN: inferior nasal; IQR, interquartile range; IR, inversion recovery; IT: inferior temporal; IV, intravenous administration; SN: superior nasal; ST: superior temporal.

Funding

This study was supported in part by Grants-in-Aid for scientific research from the Japanese Society for the Promotion of Science (JSPS KAKENHI, numbers 18K19510) to S.N.

Conflicts of Interest

Toshiaki Taoka and Rintaro Ito are the professors in the Department of Innovative Biomedical Visualization (iBMV), which is financially supported by Canon Medical Systems Corporation.

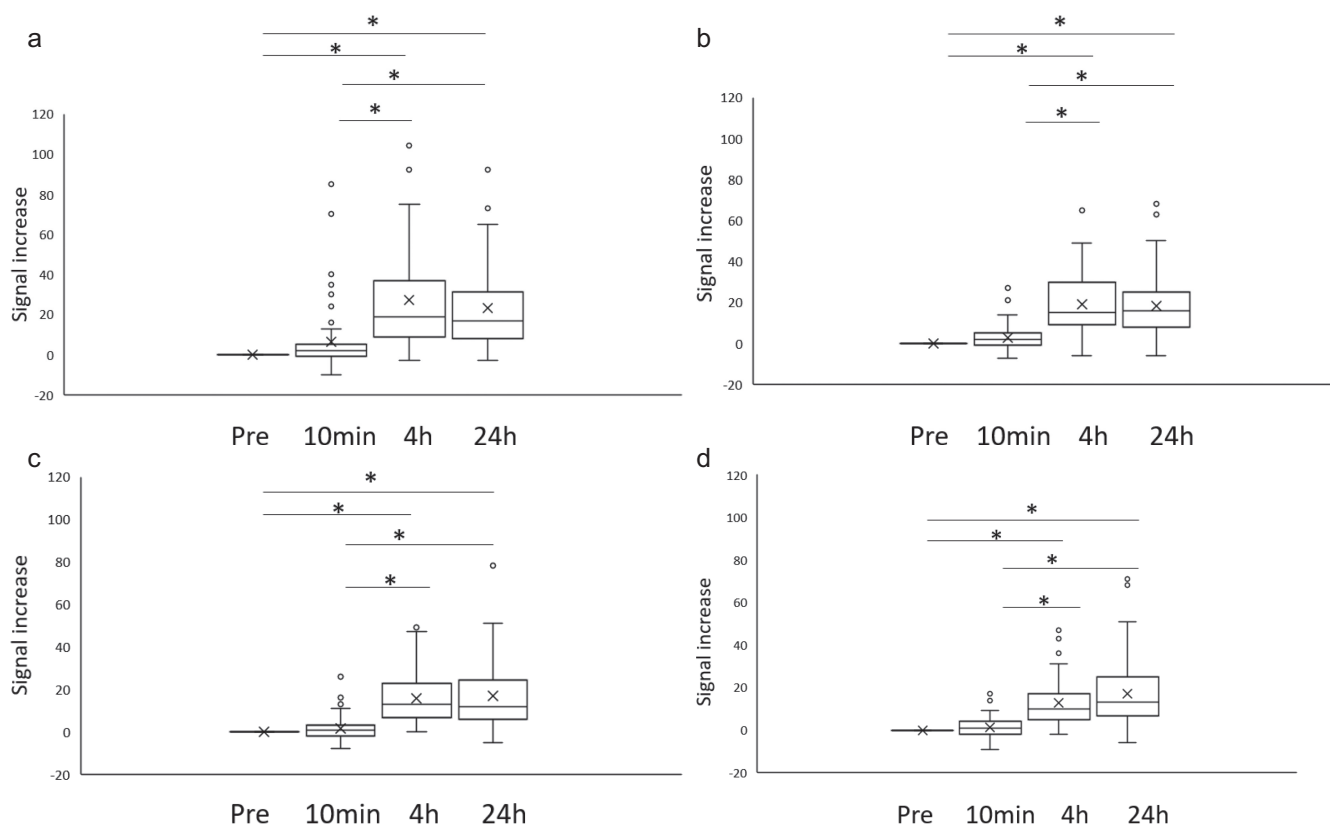


Fig. 7 The signal increase was measured in the 3D-real IR images obtained before, 10 mins, 4 hours, and 24 hours after IV-GBCA in the 33 patients with a suspicion of endolymphatic hydrops. Four ROIs (IT, IN, ST, and SN) were placed in 66 eyes of 33 patients. The time intensity trend is shown in the box-and-whisker plot for each ROI. **(a)** IT, **(b)** IN, **(c)** ST, and **(d)** SN. In the box-and-whisker plot, the lower side of the rectangle is the first quartile (25th percentile value) and the upper side is the 75th percentile value. The horizontal line in the rectangle is the median. The cross is the mean. The horizontal line under the whisker indicates the lower extreme value, and the horizontal line above the whisker indicates the upper extreme value. The upper extreme and the lower extreme are 1.5x IQR away from the edge of the box. Small circles above the whiskers are outliers. The signal intensity increase at the pre-IV-GBCA is determined as 0. The signal intensity increase was significantly higher at 4 and 24 hours compared to pre- or 10 mins after IV-GBCA in all ROIs. We used 5% as a threshold to determine statistical significance. *: Significant difference. GBCA, gadolinium-based contrast agent; IN: inferior nasal; IQR, interquartile range; IR, inversion recovery; IT: inferior temporal; IV, intravenous administration; SN: superior nasal; ST: superior temporal.

All other authors declare that they have no conflicts of interest regarding this manuscript.

References

- Lu J, Mai G, Luo Y, et al. Appearance of far peripheral retina in normal eyes by ultra-widefield fluorescein angiography. *Am J Ophthalmol* 2017; 173:84–90.
- Wang X, Xu A'min, Yi Z, et al. Observation of the far peripheral retina of normal eyes by ultra-wide field fluorescein angiography. *Eur J Ophthalmol* 2021; 31:1177–1184.
- Tawfik A, Samra YA, Elsherbiny NM, Al-Shabrawey M. Implication of hyperhomocysteinemia in Blood Retinal Barrier (BRB) dysfunction. *Biomolecules* 2020; 10:1119.
- Förster A, Wenz H, Böhme J, et al. Gadolinium leakage in ocular structures: a novel MRI finding in transient global amnesia. *J Neurol Sci* 2019; 404:63–65.
- Naganawa S, Yamazaki M, Kawai H, et al. Visualization of endolymphatic hydrops in Ménière's disease with single-dose intravenous gadolinium-based contrast media using heavily T₂-weighted 3D-FLAIR. *Magn Reson Med Sci* 2010; 9:237–242.
- Naganawa S, Kawai H, Sone M, et al. Increased sensitivity to low concentration gadolinium contrast by optimized heavily T₂-weighted 3D-FLAIR to visualize endolymphatic space. *Magn Reson Med Sci* 2010; 9:73–80.
- Naganawa S, Suzuki K, Yamazaki M, et al. Serial scans in healthy volunteers following intravenous administration of gadoteridol: time course of contrast enhancement in various cranial fluid spaces. *Magn Reson Med Sci* 2014; 13:7–13.
- Deike-Hofmann K, Reuter J, Haase R, et al. Glymphatic pathway of gadolinium-based contrast agents through the brain: overlooked and misinterpreted. *Invest Radiol* 2019; 54:229–237.
- Galmiche C, Moal B, Marnat G, et al. Delayed gadolinium leakage in ocular structures: a potential marker for age- and

- vascular risk factor-related small vessel disease? *Invest Radiol* 2021; 56:425–432.
10. Ito Y, Yamazaki I, Kikuchi Y, et al. Imaging characteristics of the postoperative globe: a pictorial essay. *Jpn J Radiol* 2016; 34:779–785.
 11. Reiter MJ, Schwoppe RB, Kini JA, et al. Postoperative imaging of the orbital contents. *Radiographics* 2015; 35:221–234.
 12. Naganawa S, Taoka T, Kawai H, et al. Appearance of the organum vasculosum of the lamina terminalis on contrast-enhanced MR imaging. *Magn Reson Med Sci* 2018; 17:132–137.
 13. Naganawa S, Kawai H, Taoka T, et al. Improved 3D-real inversion recovery: a robust imaging technique for endolymphatic hydrops after intravenous administration of gadolinium. *Magn Reson Med Sci* 2019; 18:105–108.
 14. Straatsma BR, Landers MB, Kreiger AE. The ora serrata in the adult human eye. *Arch Ophthalmol* 1968; 80:3–20.
 15. Terasaki H, Miyake Y, Awaya S. Fluorescein angiography of peripheral retina and pars plana during vitrectomy for proliferative diabetic retinopathy. *Am J Ophthalmol* 1997; 123:370–376.
 16. Nakashima T, Sone M, Teranishi M, et al. A perspective from magnetic resonance imaging findings of the inner ear: relationships among cerebrospinal, ocular and inner ear fluids. *Auris Nasus Larynx* 2012; 39:345–355.
 17. Wang X, Lou N, Eberhardt A, et al. An ocular glymphatic clearance system removes β -amyloid from the rodent eye. *Sci Transl Med* 2020; 12:eaaw3210.
 18. Naganawa S, Ito R, Nakamichi R, et al. Relationship between time-dependent signal changes in parasagittal perivenous cysts and leakage of gadolinium-based contrast agents into the subarachnoid space. *Magn Reson Med Sci* 2021; 20:378–384.